Theoretical determination of the geometric and electronic structures of oligorylenes and poli(*peri*-naphthalene)

R. Viruela-Martín, P. M. Viruela-Martín, and E. Ortí[a)]
Departamento de Química-Física, Universitat de València, Dr. Moliner 50, E-46100 Burjassot Spain

(Received 13 May 1992; accepted 11 August 1992)

We present a theoretical investigation of the electronic structure of oligorylenes (from perylene to heptarylene, including also the naphthalene molecule) and their corresponding polymer poly(*peri*-naphthalene) (PPN) using the nonempirical valence effective (VEH) method. The geometry of the unit cell used to generate the polymer is extrapolated from the PM3-optimized molecular geometries of the longest oligorylenes. That geometry shows some bond alternation along the perimeter carbon chains and a bond length of $\approx$1.46 Å is calculated for the *peri* bonds connecting the naphthalene units. The VEH one-electron energy level distributions calculated for oligorylenes are used to interpret the experimental trends reported for the first ionization potentials, redox potentials, and lowest energy optical transitions. An excellent agreement is found between theoretical estimates and experimental values. The VEH band structure calculated for an isolated chain of PPN is interpreted in terms of the molecular orbitals of naphthalene. The ionization potential, electron affinity, and bandwidths obtained for PPN suggest a large capacity to form conducting *p*- or *n*-type materials. The small band gap of 0.56 eV predicted for PPN from VEH band structure calculations is in good agreement with theoretical and experimental estimates calculated by extrapolating the data reported for the oligomers.

I. INTRODUCTION

Since the mid-70's, conducting polymers have become one of the most attracting fields in the multidisciplinary area of materials science from both basic and applied research standpoints. In the usual sense, organic polymers, even those having π-conjugated systems with mobile π electrons, are typical insulators and exhibit high electrical conductivities only after exposition to oxidizing or reducing agents.[1] Indeed, the inorganic polymer poly(sulfur nitride), $(SN)_x$, is at present the unique polymer that shows metallic conductivity (10^3 S/cm) without such a doping process.[2]

Many efforts are currently devoted to the search for organic polymers that would be intrinsically good conductors without the need for a chemical or electrochemical doping.[3–7] The study of these polymers is of particular interest because of the problem of general instability inherent to the presence of dopant species diffused among polymer chains.

Ladderlike conjugated polymers type poly(*peri*-naphthalene), PPN, were early investigated as good candidates for intrinsic conductors.[8,9] These one-dimensional graphite polymers (they consist of linearly connected benzene rings) were expected to have high electrical conductivity and excellent environmental stability because of their unique molecular structures intermediate between those of polyacetylene and graphite. Indeed, theoretical band structure calculations on regular poly(*peri*-naphthalene) predict an almost vanishing HOMO-LUMO band gap suggesting high intrinsic electrical conductivities.[10,11] Until now, the experimental verification of these predictions has been prevented by the synthetic problems that the obtention of highly regular structures involves.

Kaplan *et al.*[8,9,12] were the first to report the synthesis of highly conducting ($\sigma_{RT}\sim$250 S/cm) films of undoped PPN via the pyrolisis of a suitable perylene-based precursor. However, elemental chemical analysis of the films suggested a highly graphitized molecular structure. By using the same precursor and modifying the synthetic route of Kaplan, Iqbal *et al.*,[13] and Murakami *et al.*[14,15] obtained highly conducting fibers of an organic polymer with a H/C ratio and infrared and Raman spectroscopies consistent with PPN. Despite these results, evidence of partial graphitization was detected. For instance, XPS and Raman laser data indicated that the carbon structure of the surface layer consisted of partially graphitized amorphous carbon, while the inner phase consisted of well-formed PPN (25 to 35 naphthalene units).[15] In summary, all these synthetic efforts and others including cationic cyclization[16] and plasma polymerization[17] imply very drastic conditions that led to partially graphitized, irregular structures with a large number of defects and structurally well-defined materials could not be obtained. Hence, the experimental work does not clearly indicate whether or not chemically regular PPN would be highly conducting.

In a detailed study of PPN and its physical properties, a major problem is then caused by the difficulty in controlling its chemical forms (structure, impurities, properties regularity, $\cdots$) and by the extremely high melting points and poor solubility that do not allow purification. To avoid all these problems, Müllen *et al.*[18–20] have recently reported for the first time the synthesis of soluble, structurally well-defined oligomers (n=0–3) of PPN (see Scheme), via the high regioselective anionic cyclization of oligo(1,4-naphthylene)s synthesized previously.

a)Author to whom correspondence should be addressed.

 0021-9606/92/238470-11$006.00

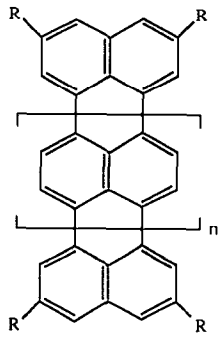

R = H (n = 0,1 ,2)
R = tBu (n = 0, 1, 2, 3)

The obtention of these soluble oligorylenes (this series is termed rylene according to the nomenclature of Clar[21]) has allowed for the first time the examination of the physical properties (uv/vis absorption and fluorescence spectra, redox activity and conductivity measurements) of this type of polycondensed aromatic hydrocarbons.[18–20] Only the physical properties of perylene ($n=0$), the first member in the series, have been previously investigated due to the lack of selective synthesis for the higher oligorylenes.

The variation of the physical properties along the homologous series of structural well-defined oligomers enables the extrapolation to the polymer and allows for a reliable estimate of the energy gap of PPN, a magnitude of prime importance in determining the intrinsic electrical conductor character. An optical gap of only 1.56 eV is measured for pentarylene ($n=3$).[19,20] This gap is significantly less than that reported for poly(*para*-phenylene) ($\approx$3.4 eV)[22] or poly(*para*-phenylene vinylene) ($\approx$2.5 eV)[23] and is comparable to that of polyacetylene ($\approx$1.5 eV).[24]

In this paper, we present a theoretical investigation of the geometric and electronic structure of a homologous series of regular oligomers of poly(*peri*-naphthalene), $(C_{10}H_4)_x$. Our main goal is to rationalize the evolution of the structural and electronic properties as the length of the oligomer increases in order to infer the properties of the polymer. The oligomers studied involve: naphthalene ($C_{10}H_8$), perylene ($C_{20}H_{12}$), terrylene ($C_{30}H_{16}$), quaterrylene ($C_{40}H_{20}$), and pentarylene ($C_{50}H_{24}$), for which experimental data are available,[18–20] and also hexarylene ($C_{60}H_{28}$) and heptarylene ($C_{70}H_{32}$) to validate the extrapolation to the polymer. It is to mention that in the framework of organic metals, oligorylenes are interesting compounds in their own right since they are reported to form a variety of charge–transfer conducting complexes.[18,19,25,26] Indeed, the first report on the electrical conductivity of charge–transfer complexes was on a perylene–bromine complex.[27]

The electronic properties and band structure of defect-free PPN have been previously investigated using different theoretical approaches,[10,11,28–33] which go from simple tight binding and perturbation MO theories[11,29,32] to minimal basis set *ab initio* calculations.[31] Especially concerned with the present work, are the VEH calculations performed by Brédas *et al.*,[10] which predict a gap of only 0.44 eV for an isolated chain of PPN. Here we reinvestigate the results of these calculations on the basis of both VEH-MO calculations on oligorylenes and VEH band structure calculations on PPN.

The paper is structured as follows. The methodology is briefly outlined in Sec. II. The geometric and electronic structures calculated for oligorylenes are presented and discussed in Sec. III and Sec. IV, respectively. Extrapolation to the polymer and the results of band structure calculations are described in Sec. V. Conclusions of this work are given in the last section.

II. METHODOLOGY

The equilibrium geometries of oligorylenes have been calculated by means of the MNDO-PM3 (modified neglect of diatomic overlap, parametric method number 3) semiempirical method[34] as implemented in the MOPAC-6.0 system of programs,[35] but slightly modified to handle large molecular systems. The MNDO-PM3 method corresponds to a reparameterization of the MNDO approach[36] in which the AM1 (Austin Model 1) form of the core–core interaction is used.[37] The suitability of the PM3 method to obtain reliable geometry estimates for aromatic hydrocarbons has been previously established.[35]

Both the molecular electronic structure of oligorylenes and the electronic band structure of poly(*peri*-naphthalene) have been investigated using the valence effective Hamiltonian (VEH) pseudopotential method. The VEH quantum-chemical technique was originally developed for molecules[38] and later extended to treat stereoregular polymers.[39,40] It takes only into account the valence electrons and is based on the use of an effective Fock Hamiltonian parameterized to reproduce the results of *ab initio* Hartree–Fock calculations without performing any self-consistent-field (SCF) process or calculating any bielectronic integral. The VEH method therefore is completely nonempirical and constitutes an specially useful tool to deal with large molecular or crystalline systems, since it yields one-electron energies of *ab initio* double-zeta quality at a reasonable computer cost. All the VEH calculations have been performed using the atomic potentials previously optimized for carbon and hydrogen.[40] The validity of the VEH approach to study the electronic structure of large π-electronic molecular systems and one-dimensional conjugated polymers has been widely illustrated in previous works.[41–43]

III. OPTIMIZED GEOMETRIES OF OLIGORYLENES

The molecular geometries of naphthalene, perylene, terrylene, quaterrylene, pentarylene, hexarylene, and heptarylene have been optimized using the PM3 method and assuming that the molecules are totally planar and have D_{2h} symmetry. In all the calculations, the gradient norm achieved is less than 0.05. Table I summarizes the bond lengths calculated for naphthalene and perylene at the PM3- and MNDO-semiempirical levels together with

TABLE I. Experimental and calculated bond lengths (in Å) for naphthalene and perylene.

Molecule	Bond	Exptl.[a]	PM3	MNDO	STO-3G[b]
Naphthalene	*a*	1.421	1.4146	1.4290	1.425
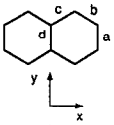	*b*	1.361	1.3685	1.3820	1.353
	c	1.425	1.4212	1.4392	1.432
	d	1.410	1.4100	1.4350	1.420
Perylene	*a*	1.415	1.4091	1.4240	1.417
	b	1.369	1.3693	1.3784	1.353
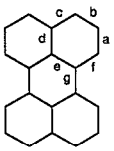	*c*	1.398	1.4202	1.4366	1.427
	d	1.421	1.4114	1.4355	1.410
	e	1.428	1.4269	1.4352	1.440
	f	1.394	1.3796	1.3969	1.367
	g	1.471	1.4617	1.4811	1.499

[a]Experimental values from uv absorption data (rotational structure) on naphthalene (Ref. 44) and x-ray diffraction data on perylene (Ref. 45).
[b]Theoretical values from Ref. 46.

available experimental data from x-ray diffraction measurements[44,45] and theoretical results from *ab initio* STO-3G calculations.[46] Table II collects the bond lengths obtained for terrylene, quaterrylene, pentarylene, and hexarylene at the PM3 level. Experimental data are only available for quaterrylene.[47] The PM3-optimized geometry computed for heptarylene is not included in Table II since it does not afford any additional data of relevance.

In order to test the reliability of the optimized geometries, we have calculated the average difference in absolute value between the experimental and calculated bond lengths reported in Table I. For the naphthalene molecule, average deviations of 0.004, 0.017, and 0.007 Å are obtained for PM3, MNDO, and STO-3G results, respectively. A similar trend is observed for the perylene molecule, for which the average deviations are calculated to be

TABLE II. PM3-optimized bond lengths (in Å) for terrylene, quaterrylene, pentarylene, and hexarylene.

Terrylene	Bond	PM3[b]	Quaterrylene[a]	Bond	PM3[b]	Exptl.[c]
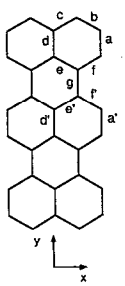	*a*	1.4088, 1.4020	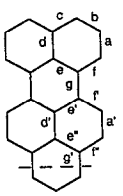	*a*	1.4088, 1.4016	1.402, 1.383
	b	1.3695		*b*	1.3695	1.369
	c	1.4200		*c*	1.4200	1.420
	d	1.4114, 1.4146		*d*	1.4114, 1.4146	1.420, 1.432
	e	1.4262, 1.4264		*e*	1.4263, 1.4261, 1.4258	1.433, 1.433, 1.432
	f	1.3802, 1.3810		*f*	1.3803, 1.3813, 1.3818	1.385, 1.385, 1.391
	g	1.4609		*g*	1.4607, 1.4599	1.468, 1.462

Pentarylene[a]	Bond	PM3[b]	Hexarylene[a]	Bond	PM3[b]
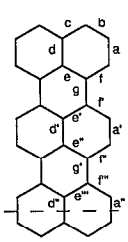	*a*	1.4088, 1.4016, 1.4012	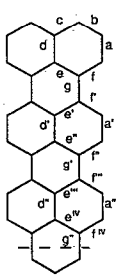	*a*	1.4089, 1.4016, 1.4012
	b	1.3695		*b*	1.3695
	c	1.4200		*c*	1.4200
	d	1.4114, 1.4146, 1.4146		*d*	1.4114, 1.4146, 1.4146
	e	1.4263, 1.4261, 1.4258, 1.4255		*e*	1.4263, 1.4261, 1.4258, 1.4255, 1.4255
	f	1.3803, 1.3814, 1.3919, 1.3821		*f*	1.3803, 1.3814, 1.3819, 1.3821, 1.3821
	g	1.4607, 1.4597		*g*	1.4607, 1.4597, 1.4595

[a]Only half of the molecule is depicted for quaterrylene, pentarylene, and hexarylene. The other half can be generated by reflection on the *xz* symmetry plane represented by a discontinuous line.
[b]PM3-optimized bond lengths for a specific type of bond are given going from the end to center of the molecule. For example, the five values reported for parameter *f* of hexarylene correspond to bond distances *f*, *f'*, *f''*, *f'''*, and *f'*^{v}, respectively.
[c]Experimental values from x-ray diffraction data (Ref. 47).

0.009 Å (PM3), 0.016 Å (MNDO), and 0.018 Å (STO-3G). These results point out that the PM3 method yields better bond length values for this type of polycondensed aromatic hydrocarbons than the MNDO method and even better than *ab initio* STO-3G calculations. The PM3 method has been therefore used to calculate the equilibrium geometries of longer oligomers.

As can be seen from Table I, both the experimental and theoretical structures reported for naphthalene indicate that the molecule is not strictly aromatic. The four bonds *b* are shorter than the remaining bonds and they have a length of 1.36–1.37 Å. This bond length value is intermediate between that of the highly localized double bonds of nonaromatic cyclopentadiene (1.342 Å)[48] and that of the fully delocalized bonds of benzene (1.399 Å).[49] The rest of C–C bonds have lengths about 1.41–1.42 Å, slightly longer than that observed for benzene. All these results suggest some degree of localization for the naphthalene molecule, although the molecule is mainly delocalized. Compared to our PM3 results and experimental data, the *ab initio* STO-3G calculations[46] tend to localize in a higher degree the geometrical structure by shortening bonds with more double bond character and lengthening bonds with more single bond character.

The bond lengths calculated for the naphthalene units forming the perylene molecule are almost equal to those obtained for the naphthalene molecule. The two bonds connecting the two naphthalene units via the carbon atoms in *peri* positions are predicted to have a length of 1.462 Å (PM3 calculations) in good agreement with the experimental x-ray value of 1.471 Å.[45] These values are considerably larger than those found for the rest of C–C bonds suggesting a poor π-delocalization between the two naphthalene units through the *peri* bonds. However, the existence of short contacts (1.808 Å after PM3 optimization) between the hydrogen atoms lying in the interannular region should be noted since they prevent a closer approaching of the naphthalene units. Indeed, the length obtained for the *peri* bonds in perylene is significantly shorter than that reported for the bond connecting the two phenyl rings in planar biphenyl ($\approx$1.50 Å),[50–52] for which similar contacts between interannular hydrogens are present. These results suggest that a more effective delocalization of the π system takes place for perylene than for biphenyl. By extrapolation, the π-electronic system of PPN could be predicted to be more effectively delocalized than that of poly(*para*-phenylene).

By comparison to naphthalene, the π-conjugation between the two naphthalene units affects more significantly the outer C–C bonds of perylene when looking along the *y* axis (see Table I for axes orientation). In passing from naphthalene to perylene, the outer bonds *f* (1.3796 Å) and *a* (1.4091 Å) of perylene experience a lengthening of 0.0111 Å and a shortening of 0.0055 Å, respectively. On the contrary, the inner bonds *e* (1.4269 Å) and *d* (1.4114 Å) are both lengthened by only 0.0057 and 0.0014 Å, respectively. These geometrical trends are confirmed by the experimental data and suggest that delocalization takes place more effectively along the atoms on the periphery of the chain.

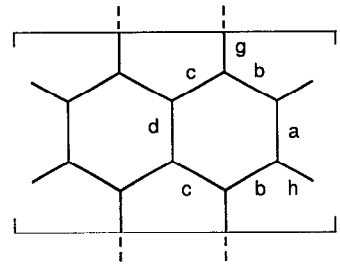

FIG. 1. PM3-optimized geometric structure for the unit cell of poly(*peri*-naphthalene). Bond lengths are given in Å and bond angles in degrees.

As can be seen from Table II, the PM3 bond lengths calculated for quaterrylene are in excellent agreement with experimental x-ray data,[47] the average deviation between theoretically calculated and experimental values being of only 0.007 Å. The analysis of the bond length values obtained for this molecule and those calculated for terrylene, pentarylene, and hexarylene leads to the same trends discussed above for perylene. The geometry obtained for the most external naphthalene units ending the oligorylene chain is the same independently of the number of these units that constitute the chain. This geometry is in fact identical to that calculated for the two naphthalene units forming the perylene molecule. In going from the end to the center of the oligorylene chain, a small but gradual modification of the bond lengths is observed. The modification trends mainly correspond to a lengthening of bonds *f* and *d* and to a shortening of bonds *a* and *d*. The length of the *peri* bonds *g* has a value of about 1.46 Å and experiences a small shortening as the length of the chain increases, i.e., as the conjugation length increases. All these trends are clearly seen for the hexarylene molecule. The small differences detected as the length of the chain increases point out that the chain end effects are mainly localized on the terminal naphthalene units.

Bond angles in oligorylenes do not differ very much from the benzene optimum value of 120°. The C–C–C angles along the outer edge of the molecule defined by the *a* bonds are all about 121°, while the angles along the inner edges defined by the *peri* bonds and the *d* bonds are of the order of 119°. These values agree with the experimental trends observed for quaterrylene.[47] C–H bond lengths are calculated to have values of 1.095–1.096 Å for the terminal naphthalene units and of 1.101 Å for the internal units.

The geometries of the central naphthalene units of pentarylene and hexarylene show a convergence to the same values of the internal parameters. The size of these oligorylenes is large enough to represent with reliability the properties of the polymer. We have therefore used the central part of the hexarylene structure to build up the geometry for the unit cell of poly(*peri*-naphthalene). The resulting unit cell is depicted in Fig. 1.

The bond distances summarized in Fig. 1 differ significantly from those previously used by Tanaka *et al.*[28] and Brédas *et al.*[10] to define the unit cell of PPN in their re-

TABLE III. VEH one-electron energy levels ($-\varepsilon_i$ in eV) obtained for naphthalene, perylene, terrylene, quaterrylene, pentarylene, and hexarylene.[a]

	Naphthalene		Perylene		Terrylene		Quaterrylene		Pentarylene		Hexarylene	
LUMO	$2b_{2g}^*$	3.56	$3b_{2g}^*$	4.41	$4b_{2g}^*$	4.75	$5b_{2g}^*$	4.92	$6b_{2g}^*$	5.03	$7b_{2g}^*$	5.11
HOMO	$1a_u$	8.21	$2a_u$	7.19	$3a_u$	6.78	$4a_u$	6.57	$5a_u$	6.44	$6a_u$	6.35
	$2b_{1u}$	9.10	$3b_{3g}$	9.07	$3b_{2g}$	8.28	$4b_{2g}$	7.71	$5b_{2g}$	7.35	$6b_{2g}$	7.10
	$1b_{3g}$	10.37	$3b_{1u}$	9.16	$4b_{3g}$	8.77	$6b_{3g}$	8.57	$4a_u$	8.30	$5a_u$	7.91
			$2b_{3g}$	9.21	$5b_{1u}$	9.07	$3a_u$	8.86	$6b_{3g}$	8.45	$9b_{3g}$	8.38
			$2b_{2g}$	9.27	$3b_{3g}$	9.12	$5b_{3g}$	9.07	$8b_{1u}$	9.07	$5b_{2g}$	8.70
					$4b_{1u}$	9.19	$6b_{1u}$	9.10	$5b_{3g}$	9.09	$9b_{1u}$	8.91
					$2a_u$	9.67	$4b_{3g}$	9.16	$7b_{1u}$	9.10	$8b_{3g}$	9.06
							$5b_{1u}$	9.20	$6b_{1u}$	9.16	$8b_{1u}$	9.08
							$4b_{1u}$	9.54	$4b_{3g}$	9.18	$7b_{3g}$	9.11
							$3b_{2g}$	9.88	$4b_{2g}$	9.21	$7b_{1u}$	9.16
									$5b_{1u}$	9.24	$6b_{3g}$	9.19
									$3a_u$	10.00	$6b_{1u}$	9.23
											$4a_u$	9.44
											$5b_{3g}$	9.67

[a]The lowest unoccupied molecular orbital (LUMO) and the highest occupied molecular orbitals of energy above $\varepsilon_i = -10.0$ eV are included. All orbitals are of π nature. They have been numbered starting with the lowest-lying valence orbital.

spective band structure calculations. On the basis of CNDO/2 calculations, Tanaka *et al.* suggest that the most stable structure of PPN corresponds to a graphitized version of planar poly(*para*-phenylene) rather than a chain made up from the connection of perylene molecules.[28] They predict highly localized double bonds in the outer edge of the chain ($a=1.356$ Å), all the other bond lengths being about 1.425 Å. This structure is also used by Bakhshi *et al.* in their *ab initio* band structure calculations.[31] Brédas *et al.* define a unit cell similar to that of Tanaka *et al.*. They use a bond length of 1.370 Å for bonds *a* all the other bonds, including the *peri* bonds, having a length of 1.423 Å.[10] The main differences between these unit cells and the geometry we propose in Fig. 1 are (i) bonds *a* are too short, we suggest a length of about 1.40 Å; (ii) bonds *b* are too long, we obtain a value of about 1.38 Å; and (iii) *peri* bonds are too short, we predict a length of about 1.46 Å.

IV. ELECTRONIC STRUCTURE OF OLIGORYLENES

The one-electron energy level distributions calculated for oligorylenes, from naphthalene to hexarylene, using the VEH method and the PM3-optimized geometries presented in Tables I and II are reported in Table III. Only the lowest unoccupied molecular orbital (LUMO) and the highest occupied molecular orbitals with energies above -10.0 eV are included in Table III because they determine the most interesting electronic properties. All these orbitals are of π nature, the first occupied σ orbitals appearing below -10.1 eV. They have been classified according to the D_{2h} point group which identifies the molecular symmetry in all cases. As indicated in Tables I and II, we have taken the long molecular axis as the y axis and the short molecular axis as the x axis.

The splitting that the highest three occupied molecular orbitals of naphthalene experience when passing to perylene, terrylene, and quaterrylene is schematically shown in Fig. 2. The particular splitting undergone by the highest occupied molecular orbital (HOMO) is displayed in more detail in Fig. 3, where the atomic orbital contributions are depicted. The correlations presented both in Fig. 2 and Fig. 3 have been inferred from a detailed analysis of the atomic orbital composition of the respective molecular orbitals.

Table III and Figs. 2 and 3 indicate that the HOMO corresponds, in all cases, to a level of a_u symmetry. It is important to note, that this level has the same atomic orbital patterns for all the oligorylenes. As shown in Fig. 3, the a_u HOMOs involve contributions from all the carbons atoms except from those forming the central edge of the molecule along the y axis.

A monotonous destabilization of the HOMO level is observed in Table III and Fig. 2 as the length of the oligorylene increases. This energetic destabilization accords with the gradual lowering experimentally observed for the first ionization potential. Following Koopmans' theorem, the first ionization potential of naphthalene corresponds to the ejection of an electron from the $1a_u$ HOMO and is calculated to be 8.21 eV in very good agreement with the experimental gas-phase UPS estimate of 8.15 eV.[53] For perylene, the $2a_u$ HOMO is calculated to lie at -7.19 eV, which is about 1 eV above the HOMO of naphthalene. This is good correspondence with the first ionization potential of 6.79 eV measured in gas phase for perylene,[54] which is about 1.2 eV lower than that of naphthalene. For longer oligorylenes, the energy of the a_u HOMO continues to increase and ionization energies of 6.78, 6.57, 6.44, and 6.35 eV are predicted for terrylene, quaterrylene, pentarylene, and hexarylene, respectively. The values calculated for terrylene and quaterrylene are in good agreement with the gas-phase UPS estimates of 6.42 and 6.11 eV, respectively.[55] However, it is to be noted that the theoretically calculated values decrease more slowly than the experimentally measured values. While for naphthalene we find an excellent quantitative agreement, the ionization potential calculated for quaterrylene (6.57 eV) overestimates by 0.46 eV the experimental value (6.11 eV).

The rise in energy of the HOMO level along the series of oligorylenes is an expected result for conjugated oligo-

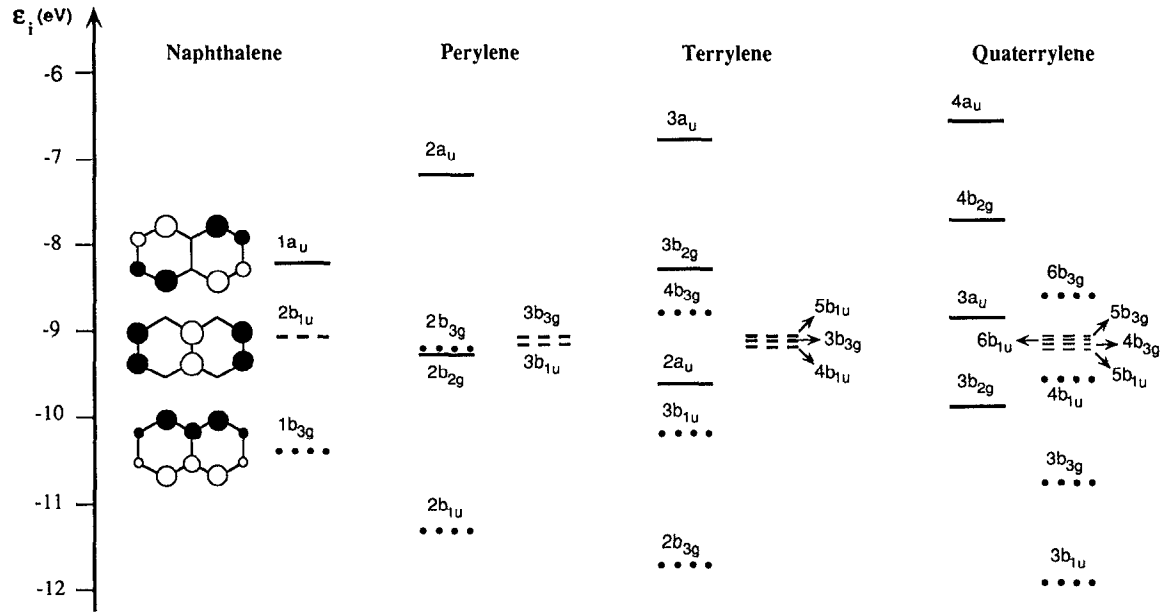

FIG. 2. Correlation diagram showing the splitting of the highest three occupied molecular orbitals of naphthalene when passing to perylene, terrylene, and quaterrylene. Levels deriving from $1a_u$, $2b_{1u}$, and $1b_{3g}$ molecular orbitals of naphthalene are denoted by continuous (—), broken (- - -), and dotted (···) lines, respectively. One-electron energies (ε_i) and symmetries correspond to those given in Table III. All the orbitals are of π type.

mers and can be understood in terms of the atomic orbital patterns sketched in Fig. 3. The HOMO of naphthalene can be visualized as constituted by the $1a_2$ HOMOs of two *cis*-butadiene fragments with no interaction through the central C–C bond. In a first-order perturbation scheme, the $2a_u$ HOMO of perylene can be considered as the result of the antibonding interaction through the *peri* carbons of the $1a_u$ HOMOs of two naphthalene units. This antibonding interaction causes the destabilization of the HOMO of perylene (−7.19 eV) with respect to that of naphthalene (−8.21 eV), while the respective bonding interaction gives rise to the $2b_{2g}$ molecular orbital of perylene located at −9.27 eV.

Similar arguments can be used to interpret the progressive destabilization of the HOMO along the series of oligorylenes. As can be seen from Fig. 3, two antibonding interactions through the *peri* carbons are present in the $3a_u$ HOMO (−6.78 eV) of terrylene, three in the $4a_u$ HOMO (−6.57 eV) of quaterrylene, and so on. The rise in energy for these levels is less important than for perylene due to the fact that the terminal naphthalene units interact less strongly than the central units. On the other hand, the $1a_u$ orbitals of the three naphthalene fragments forming terrylene interact in a totally bonding way to give rise to the $2a_u$ level at −9.67 eV or in a nonbonding way to obtain the $3b_{2g}$ level at −8.28 eV, which shows no contribution from the *peri* carbons of the central naphthalene unit. In the case of quaterrylene the totally bonding interaction through the *peri* bonds gives rise to the $3b_{2g}$ level at −9.88 eV, while intermediate interactions lead to the $3a_u$ (two bonding and one antibonding) level at −8.86 eV and to the $4b_{2g}$ (one bonding and two antibonding) level at −7.71 eV. This splitting scheme is reproduced for longer members of the oligomer series, a nonbonding molecular orbital with energy similar to that of the $1a_u$ HOMO of naphthalene always appearing for oligomers with an odd number of naphthalene units.

The VEH results indicate that the extension of the conjugated system by linear connection of naphthalene units through *peri* positions causes a continuous destabilization of the highest occupied molecular orbital and, consequently, a decrease in the first ionization potential of the oligorylene. These results agree with the experimental trends observed by Clar *et al.* in their extensive work on polycondensated benzenoid hydrocarbons.[56,57] Since oxidation involves removing an electron from the HOMO, it is reasonable to expect that oligomers with higher lying HOMOs have lower oxidation potentials. In this way, the relative stabilities of the HOMO levels predicted by the VEH method justify the decrease of the first oxidation potential as the size of the oligomer increases measured by Müllen *et al.* .[18,19,58] For example, a decrease of 0.30 eV is reported for the first oxidation potential in going from perylene (0.75 eV) to terrylene (0.45 eV) in very good agreement with the destabilization of 0.41 eV calculated for the HOMO level in passing from perylene to terrylene.

As can be seen from Fig. 2, the second-highest occupied molecular orbital of naphthalene ($2b_{1u}$) is formed by three noninteracting ethylene π bonds located on the central and lateral C–C bonds. The atomic orbital composition of this orbital and in particular the zero contributions of the *peri* carbons determine the nonbonding character of the interaction between the $2b_{1u}$ orbitals of the naphthalene units constituting the oligorylenes. As a result, a group of close-lying molecular orbitals appears for all oligorylenes about −9.10 eV, i.e., the energy calculated for the $2b_{1u}$

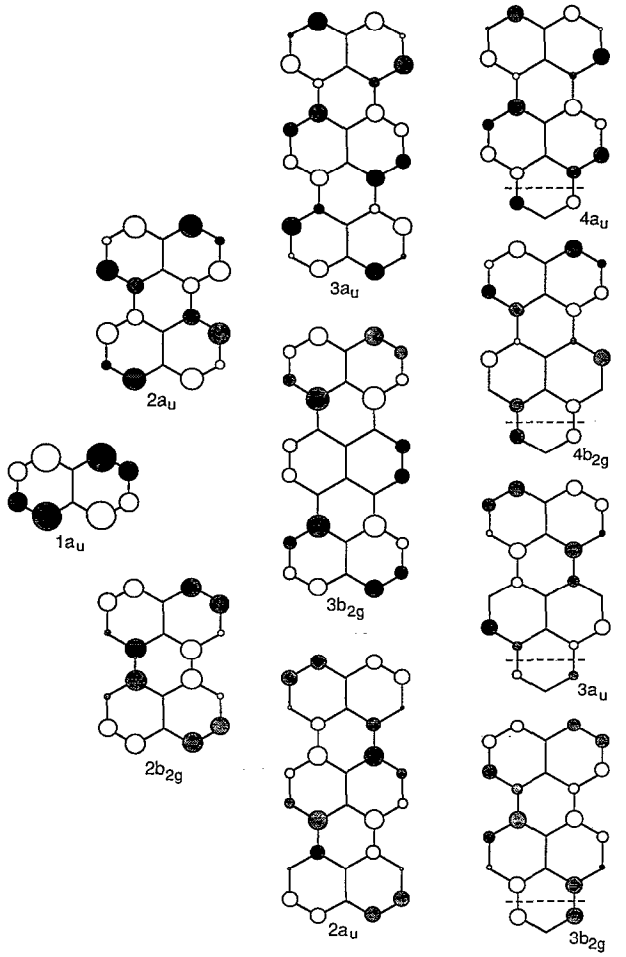

FIG. 3. Schematic drawing showing the atomic orbital (AO) composition of the highest occupied molecular orbitals of perylene, terrylene, and quaterrylene resulting from the interaction of the HOMO of naphthalene units. The size of the circles is proportional to the magnitude of the AO coefficients. A white area indicates a positive value for the upper lobe of the p_π AO, while a grey area indicates a negative value. Only half of the molecule is depicted for quaterrylene. MO symmetries correspond to those given in Table III and Fig. 2.

level of naphthalene (see Fig. 2). The $1b_{3g}$ molecular orbital of naphthalene undergoes a splitting scheme similar to that discussed above for the $1a_u$ HOMO as a consequence of the nonzero contributions on the *peri* carbons.

We turn now to discuss the optical properties displayed by the oligorylenes in order to elucidate the evolution of the energy gap that separates the occupied from the unoccupied energy levels and its possible extrapolation to the polymer. The energy gap is a quantity of great significance for a polymer since it mainly determines the intrinsic conductivity properties. In the case of discrete molecules (oligomers), it corresponds in a first approach to the HOMO/LUMO energy difference. One of the ways of characterizing it experimentally is to measure the potential difference between the first stage of reduction and oxidation. Alternatively, one can determine the energy of the longest wavelength optical transition.[18–20]

Table IV summarizes the values of the HOMO/LUMO energy differences experimentally determined by

TABLE IV. Experimentally determined and theoretically calculated HOMO/LUMO energy differences ΔE (in eV) for PPN oligomers. The results in the first three columns are taken from Müllen *et al.* (Refs. 18–20) and correspond to tetra-tertbutyl derivatives. The fourth column collects results from Clar (Ref. 59).

Molecule	ΔE_{el}[a]	ΔE_{opt}[b]	ΔE_{opt}[c]	ΔE_{opt}[d]	ΔE_{VEH}[e]
Perylene	2.77	2.67		2.85	2.78
Terrylene	2.00	2.14	2.02	2.21	2.03
Quaterrylene	1.64	1.80	1.58	1.85	1.65
Pentarylene		1.56	1.32		1.40
Hexarylene					1.24
Heptarylene					1.12
PPN		0.98[f]	0.92[f]		0.42[g]

[a]Difference between the electrochemically determined redox potentials for the radical cation and radical anion.
[b]Energy of the longest wavelength optical transition, determined at 1/10 of the maximum absorption in 1,4-dioxane solution.
[c]Same as item *b* but for films obtained by evaporation onto glass plates.
[d]Energy of longest wavelength $S_0 \rightarrow S_1$ (p band) transitions according to Clar (Ref. 59).
[e]Calculated values using the VEH method. This work.
[f]Value extrapolated to the polymer by using the Padé approximation (Ref. 20).
[g]Value extrapolated to the polymer by using the polynonial $y=a+b/N+c/N^2+d/N^3$, N being the number of naphthalene units forming the oligomer. The VEH HOMO/LUMO energy gap obtained for naphthalene (4.65 eV) is also used for the fitting.

electrochemical[18,19] and optical[18–20,59] measurements and theoretically estimated by using the VEH method. The VEH values are calculated by simple differences between the one-electron energies of the HOMO and LUMO molecular levels. It is to be noted that compared to standard *ab initio* Hartree–Fock calculations, the VEH method provides good estimates for the lowest energy optical transitions. As previously discussed,[60] this feature is due to the fact that the VEH parameterization is not contaminated by any information coming from the unoccupied Hartree–Fock molecular orbitals which are always calculated to be too diffuse. Effectively, the HOMO/LUMO energy gaps predicted by the VEH method are in excellent agreement with the experimental values, especially with those estimated from the difference between cyclovoltammetrically determined redox potentials ($\Delta E = E^{l}_{1/2}(\mathrm{ox}) - E^{l}_{1/2}(\mathrm{red})$).[18,19]

The VEH method predicts a decrease of the HOMO/LUMO energy gap as the degree of annelation increases. While an energy gap of 2.78 eV is calculated for perylene in good accord with the electrochemical (2.77 eV) and optical (2.67 eV) estimates, a gap of only 1.12 eV is obtained for heptarylene. This energy gap is even smaller than that measured for polyacetylene ($\simeq$1.5 eV).[24] The narrowing of the HOMO-LUMO energy gap is in good agreement with the bathochromic shift observed for the longest wavelength transition in going from perylene to pentarylene.[18–20] This narrowing is due to the progressive increase of the energy of the HOMO and the parallel decrease of the energy of the LUMO as the length of the oligomer increases (see Table III). The destabilization of the HOMO has already been discussed. The LUMO corresponds, in all cases, to a π^* molecular orbital of b_{2g}

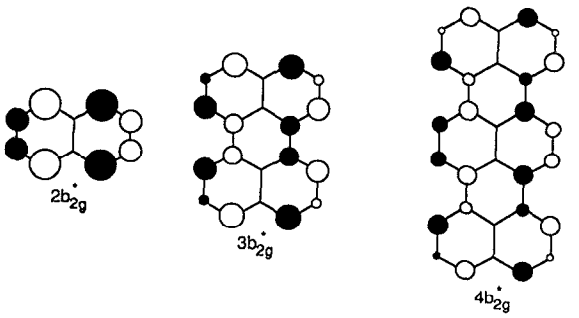

FIG. 4. Schematic drawing showing the atomic orbital composition of the lowest unoccupied molecular orbitals of naphthalene, perylene, and terrylene. The size of the circles is proportional to the magnitude of the AO coefficients. MO symmetries correspond to those given in Table III.

symmetry. The continuous stabilization of the LUMO can be understood from Fig. 4, where the atomic orbital composition of this orbital is depicted for naphthalene, perylene, and terrylene. Similarly to the HOMO, the LUMO level has no contribution from the carbon atoms located in the middle of the molecule along the long axis. For perylene, the LUMO can be visualized as resulting from the bonding interaction of the $2b_{2g}$ LUMOs of the two naphthalene units. The LUMO of terrylene involves two bonding interactions of the same type through the *peri* bonds. These bonding interactions determine the monotonous stabilization of the LUMO level as the length of the oligomer increases. Energy stabilizations of 0.34 and 0.17 eV are calculated when passing from perylene to terrylene and from terrylene to quaterrylene. These values are in excellent correlation with the variations of 0.34 and 0.22 V measured cyclovoltammetrically for the first reduction potential when passing from perylene (-1.99 V) to terrylene (-1.65 V) and from terrylene to quaterrylene (-1.43 V).[58]

V. ELECTRONIC STRUCTURE OF PPN

As a first approach to the electronic properties of poly(*peri*-naphthalene), we have extrapolated the VEH results obtained for oligorylenes by fitting them to a polynomial in inverse powers of N ($y=a+b/N+c/N^2+d/N^3$), N being the number of naphthalene units forming the oligomer. The extrapolation for an infinite chain ($N=\infty$) leads to one-electron energies of -5.91 and -5.49 eV for the HOMO and LUMO levels and, as a result, an HOMO/LUMO energy gap of only 0.42 eV is predicted for PPN. This energy gap is almost identical to the value obtained by Brédas *et al.* (0.44 eV) from VEH band structure calculations on PPN,[10] and underestimates by $\approx$0.5 eV the value extrapolated by Müllen *et al.* (0.92–0.98 eV) from optical absorption measurements.[20]

As a second approach, we have calculated the electronic valence band structure for an infinite chain of stereoregular PPN by using the VEH method and the unit cell proposed in Fig. 1. The resultant band structure is displayed in Fig. 5, where only the higher-lying valence bands and the lowest three unoccupied bands are shown. As performed above for oligorylenes, we focus on the one-electron energy levels of π nature. In this way, Fig. 6 sketches the atomic orbital patterns of the five occupied π bands (π_1 to π_5) and the lowest unoccupied π band (π_6) at the center ($k=0$) of the Brillouin zone.

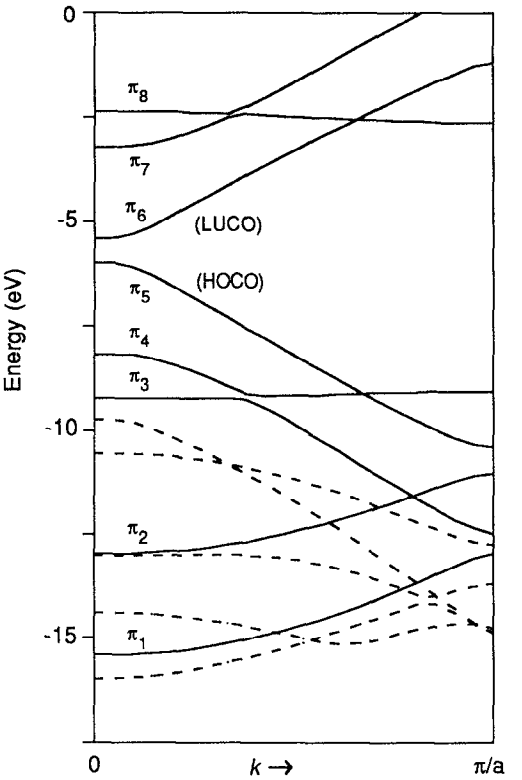

FIG. 5. VEH band structure of poly(*peri*-naphthalene). Only the highest occupied and lowest three unoccupied bands are displayed. Broken and solid lines represent σ and π bands, respectively.

Bands π_1 to π_6 show a one-to-one correspondence with the molecular orbitals of naphthalene (compare Fig. 6 with Figs. 2 and 4), and the band structure of PPN can be easily interpreted in terms of the MOs of the monomer. For example, band π_5 clearly originates in the interaction of the $1a_u$ HOMO levels of the naphthalene units. The antisymmetric character of this molecular orbital with respect to the plane perpendicular to the chain axis (see Fig. 2) results in an antibonding interaction at $k=0$ (in-phase trans-

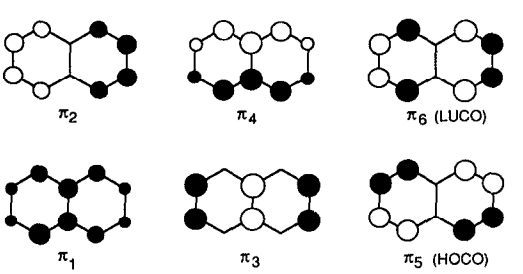

FIG. 6. Schematic drawing showing the atomic orbital composition at $k=0$ of the five occupied π bands (π_1 to π_5) and lowest unoccupied π band (π_6) of poly(*peri*-naphthalene).

lation) and in a bonding interaction at $k=\pi/a$ (out-of-phase translation). These facts determine that band π_5 goes down in energy toward $k=\pi/a$ and that the highest occupied crystal orbital (HOCO) corresponds to $k=0$ (see Fig. 5). The opposite occurs for band π_6 (which goes up in energy toward $k=\pi/a$) due to the symmetric character of the $2b_{2g}$ LUMO of naphthalene with respect to the plane perpendicular to the chain axis (see Fig. 4). As a result, the lowest unoccupied crystal orbital (LUCO) also appears at $k=0$. The minimum band gap for PPN therefore corresponds to a direct energy gap at the center ($k=0$) of the Brillouin zone, as it is also the case for poly(*para*-phenylene).[61]

Bands π_3 and π_4 result from the mixing of the $2b_{1u}$ and $1b_{2g}$ molecular orbitals of naphthalene (see Figs. 2 and 6). The flat sections of these bands correspond to the interaction of the $2b_{1u}$ levels which have zero contributions on the carbon atoms connecting the naphthalene units. The disperse sections originate in the interaction of the $1b_{2g}$ levels which show the largest contributions on those carbon atoms. The mixing of the atomic patterns of bands π_3 and π_4 is a result of the internal symmetry of PPN. As can be inferred from Fig. 6, these two bands are symmetric with respect to the mirror plane of symmetry running along the chain axis. The fact that they have the same symmetry determines the avoided crossing between them around $k=\pi/3a$ and, as a consequence, the exchange of their atomic patterns. Bands π_2 and π_5 are antisymmetric with respect to that mirror plane and have no restriction to cross bands π_3 and π_4, respectively, showing no change in their atomic patterns.

The main difference between the band structure displayed in Fig. 5 and that previously reported by Brédas *et al.*[10] is that the HOCO and the LUCO are interchanged. As can be seen from Fig. 6, our VEH calculations predict a bonding character for the *b* bonds and an antibonding character for the *a* bonds in the HOCO and the contrary is observed in the LUCO (see Fig. 1 for bond labels). These trends are exactly the opposite to those obtained by Brédas *et al.*[10] and Bakhshi *et al.*[31] and can be explained on the basis of the different geometry used to define the unit cell. In the unit cell we use to generate the polymer bonds *b* (1.3821 Å) are shorter than bonds *a* (1.4012 Å) and especially than *peri* bonds (1.4595 Å). These bond distances suggest that the HOCO and LUCO bands of PPN should be considered as formed by two interacting *trans-cis*oid polyacetylene chains instead of the two *cis-trans*oid polyacetylene chains previously proposed.[10,31] The differences between these two kinds of polyacetylene chains are depicted in Fig. 7.

Table V summarizes the VEH electronic properties calculated for PPN together with those previously reported by Brédas *et al.*[10] and Bakhshi *et al.*[31] The VEH electronic properties obtained by Brédas *et al.* for the most widely studied hydrocarbon conducting polymers such as poly(*para*-phenylene) (PPP),[61] poly(*para*-phenylene vinylene) (PPV),[62] and all-*trans* polyacetylene (PA)[40] are also included in Table V for the sake of comparison. Note that the VEH ionization potential (IP) values are scaled down by 1.9 eV to take into account the solid-state polarization energy. The 1.9 correction factor results from the scaling of the VEH theoretical IP value to the experimental value in PA (Ref. 40) and has been successfully used in previous VEH calculations.[61,62]

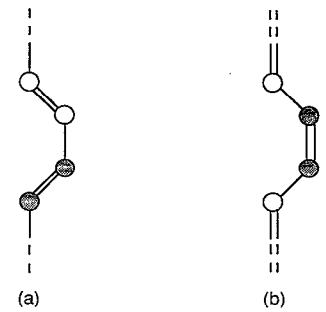

FIG. 7. Schematic drawing showing the atomic orbital composition at $k=0$ for the HOCO bands of *trans–cis*oid (a) and *cis–trans*oid (b) polyacetylene.

Despite the differences in the unit cells used to generate the polymer, the values we obtain for the electronic properties of PPN are almost identical to those reported by Brédas *et al.*[10] This feature can be understood as a result of the fact that the total length of the unit cell we use in the VEH calculations (4.284 Å) is only slightly larger than that used by Brédas *et al.* (4.269 Å).

The solid-state ionization potential calculated for PPN (4.08 eV) is significantly lower than those reported for PPP (5.6 eV),[61] PPV (5.1 eV),[62] and even for PA (4.7 eV).[40] Moreover, the VEH value of 4.08 eV is expected to be too large by about 0.5 eV since, as discussed in Sec. IV, the VEH ionization potentials calculated for oligorylenes decrease with the chain length more slowly than the experimental gas-phase values do. The VEH electron affinity calculated for PPN (3.52 eV) is of the order of that obtained for PA (3.3 eV)[40] and larger than those reported for

TABLE V. Ionization potentials (IP), electron affinities (EA), band gap values (E_g), and HOCO bandwidths (HOBW) of poly(*peri*-naphthalene) (PPN), poly(*para*-phenylene) (PPP), poly(*para*-phenylene vinylene) (PPV), and all-*trans* polyacetylene (PA). All values are given in eV.

	IP	EA	E_g	HOBW
PPN[a]	4.08	3.52	0.56	4.41
PPN[b]	4.00	3.60	0.44	4.40
PPN[c]	8.39	3.88	4.51	4.59
PPP[d]	5.6	2.1	3.5	3.5
PPV[e]	5.1	2.6	2.5	2.8
PA[f]	4.7	3.3	1.4	6.5

[a]VEH calculations, this work.
[b]VEH calculations, from Ref. 10.
[c]*Ab initio* Hartree–Fock calculations, from Ref. 31.
[d]VEH calculations from Ref. 61.
[e]VEH calculations from Ref. 62.
[f]VEH calculations from Ref. 40.

PPP (2.1 eV)[61] and PPV (2.6 eV).[62] The low value of the ionization potential and the high value of the electron affinity, together with the large widths of the HOCO (4.41 eV) and LUCO (4.23 eV) bands, support the large capacity to form conducting *p*- and *n*-type materials expected for PPN.

Finally, we predict a band gap of only 0.56 eV for PPN. This value is slightly larger than that we obtain by extrapolating the VEH results on oligorylenes (0.42 eV) and that reported by Brédas *et al.* (0.44 eV),[10] but it is still significantly lower than that obtained for PA (1.4 eV).[40] The agreement with the experimental estimates of Müllen *et al.* (0.92–0.98 eV)[20] is quite good, but our theoretical value seems to be too small by $\approx$0.4 eV. However, it is to note that the experimental estimates are based on extrapolations using the optical data measured for a few number of oligorylenes (see Table IV). Thus while Tyutyulkov *et al.* [33] predict an energy gap of 1.19 eV for PPN using the data reported for perylene, terrylene, and quaterrylene, Müllen *et al.*[20] obtain a value of only 0.92–0.98 eV using the data reported for terrylene, quaterrylene, and pentarylene. Tyutyulkov *et al.*[33] also predict an extrapolated energy gap as large as 1.32 eV using the electrochemical data collected in Table IV. Although these data perfectly match the VEH energy gaps calculated for perylene, terrylene, and quaterrylene, the extrapolation we perform of the VEH values from naphthalene to hexarylene leads to a quite different estimate for the energy gap of PPN (0.42 eV). All these results suggest that experimental data on longer oligorylenes would be desirable to obtain a reliable estimate of the band gap of PPN. In any case, the important point to emphasize is that nowadays there are enough experimental and theoretical data to support a band gap estimate of about 0.6–0.9 eV for PPN. It is to mention that these values are mainly inferred for isolated PPN chains. Brédas *et al.*[10] theoretically predict a further narrowing of 0.15 eV for the band gap of PPN in the solid state due to the interchain interactions resulting from the close packing expected for PPN chains. This prediction is supported by the smaller band gaps experimentally obtained for oligorylenes in the solid state (see Table IV). In conclusion, the band gaps calculated from both experimental and theoretical data are small enough to expect very interesting intrinsic conduction properties for nongraphitized poly(*peri*-naphthalene).

VI. SUMMARY AND CONCLUSIONS

We have investigated the geometric and electronic structure of a homologous series of oligorylenes in order to gain some insight into the structural and electronic peculiarities of poly(*peri*-naphthalene) (PPN). The PM3-optimized geometries of oligorylenes suggest that the π-electronic system of PPN is more effectively delocalized than that of the related hydrocarbon polymer poly(*para*-phenylene). This delocalization seems to take place preferentially along the carbon atoms on the perimeter of the chain. The geometry extrapolated for the unit cell of PPN shows some bond alternation along the peripheral carbon chains which can be regarded as *trans-cis*oid polyacetylene chains.

The one-electron energy level distributions calculated for oligorylenes by using the valence effective Hamiltonian (VEH) nonempirical technique have been analyzed in very detail. A continuous destabilization of the HOMO level and stabilization of the LUMO level are obtained as the size of the oligorylene increases. As a result, a decrease of the first ionization potential and a narrowing of the HOMO/LUMO energy gap are both observed in going along the series. These trends support the experimental decrease observed for the oxidation potential and the bathchromic shift measured for the lowest energy electronic transition. A very good agreement is found between theory and experiment in predicting electronic properties such as ionization potentials, redox potentials, and HOMO/LUMO energy gaps.

The VEH results obtained from band structure calculations on PPN are consistent with the conclusions inferred from the geometric and electronic properties of oligorylenes. Compared to the most studied hydrocarbon conducting polymers, PPN is calculated to have a low ionization potential (4.08 eV), a large electron affinity (3.52 eV), and large widths for the valence (4.41 eV) and conduction (4.23 eV) bands. All these features determine the large capacity expected for PPN to form conducting *p*- and *n*-type materials. The small band gap of 0.56 eV obtained for PPN is in good agreement with experimental estimates obtained by extrapolating optical data on oligorylenes.

ACKNOWLEDGMENTS

The authors acknowledge Professor F. Tomás for the implementation of enlarged versions of the MOPAC system of programs. They thank the CIUV (Centro de Informática de la Universitat de València) for the use of their computing facilities. This work has been supported by the DGICYT Projects No. PS88-0112 and OP90-0042.

[1] H. Shirakawa, E. J. Louis, A. G. MacDiarmid, C. K. Chiang, and A. J. Heeger, J. Chem. Soc., Chem. Commun. **578** (1977); C. K. Chiang, C. R. Fincher, Y. W. Park, A. J. Heeger, H. Shirakawa, E. J. Louis, S. C. Gau, and A. G. MacDiarmid, Phys. Rev. Lett. **39**, 1098 (1977).
[2] V. V. Walatka, M. M. Labes, and J. H. Perlstein, Phys. Rev. Lett. **31**, 1139 (1973).
[3] F. Wudl, M. Kobayashi, and A. J. Heeger, J. Org. Chem. **49**, 3381 (1984); M. Kobayashi, N. Colaneri, M. Boysel, F. Wudl, and A. J. Heeger, J. Chem. Phys. **82**, 5717 (1985); N. Colaneri, M. Kobayashi, A. J. Heeger, and F. Wudl, Synth. Met. **14**, 15 (1986).
[4] J. L. Brédas, J. Chem. Phys. **82**, 3808 (1985); J. L. Brédas, A. J. Heeger, and F. Wudl, *ibid.* **85**, 4673 (1986); J. L. Brédas, Synth. Met. **17**, 115 (1987).
[5] J. M. Toussaint, F. Wudl, and J. L. Brédas, J. Chem. Phys. **91**, 1783 (1989).
[6] J. M. Toussaint and J. L. Brédas, J. Chem. Phys. **94**, 8122 (1991).
[7] Y. S. Lee and M. Kertesz, Int. J. Quantum Chem. Symp. **21**, 163 (1987); J. Chem. Phys. **88**, 2609 (1988); M. Kertesz and Y. S. Lee, J. Phys. Chem. **91**, 2690 (1987); Y. S. Lee, M. Kertesz, and R. L. Elsenbaumer, Chem. Mater. **2**, 526 (1990); J. Kurti, P. R. Surján, and M. Kertesz, J. Am. Chem. Soc. **113**, 9865 (1991).
[8] M. L. Kaplan, P. H. Schmidt, C. H. Chen, and W. M. Wahsh Jr., Appl. Phys. Lett. **36**, 867 (1980).
[9] P. H. Schmidt, D. C. Joy, M. L. Kaplan, and W. L. Fieldmann, Appl. Phys. Let. **40**, 93 (1982); S. R. Forrest, M. L. Kaplan, P. H. Schmidt,

T. Venkatesan, and A. J. Lovinger, *ibid* **41**, 708 (1982).
[10] J. L. Brédas and R. H. Baughman, J. Chem. Phys. **83**, 1316 (1985).
[11] I. Bozovic, Phys. Rev. B **32**, 8136 (1985).
[12] M. L. Kaplan, S. R. Forrest, P. H. Schmidt, and T. Venkatesan, J. Appl. Phys. **55**, 732 (1984).
[13] Z. Iqbal, D. M. Ivory, J. Marti, J. L. Brédas, and R. H. Baughman, Mol. Cryst. Liq. Cryst. **118**, 103 (1985); Z. Iqbal, C. Maleysson, and R. H. Baughman, Synth. Met. **15**, 161 (1986).
[14] M. Murakami and S. Yoshimura, J. Chem. Soc. Chem. Commun. 1649 (1984); Mol. Cryst. Liq. Cryst. **118**, 95 (1985).
[15] M. Murakami, S. Iijima, and S. Yoshimura, J. Appl. Phys. **60**, 3856 (1986).
[16] J. H. Banning and M. B. Jones, Polym. Prepr. (Am. Chem. Soc. Div. Polym. Chem.) **28**, 223 (1987).
[17] M. Murashima, K. Tanaka, and T. Yamabe, Synth. Met. **33**, 373 (1989).
[18] A. Bohnen, K.-H. Koch, W. Lüttke, and K. Müllen, Angew. Chem. Int. Ed. Engl. **29**, 525 (1990).
[19] K.-H. Koch, U. Fahnenstich, M. Baumgarten, and K. Müllen, Synth. Met. **42**, 1619 (1991).
[20] K.-H. Koch and K. Müllen, Chem. Ber. **124**, 2091 (1991).
[21] E. Clar, Chem. Ber. **81**, 52 (1948).
[22] L. W. Shacklette, H. Eckhardt, R. R. Chance, G. C. Miller, D. M. Ivory, and R. H. Baughman, J. Chem. Phys. **73**, 4098 (1980).
[23] R. H. Friend, D. D. C. Bradley, and P. D. Townsend, J. Phys. D **20**, 1367 (1987).
[24] R. R. Chance, D. S. Boudreaux, H. Eckhardt, R. L. Elsenbaumer, J. E. Frommer, J. L. Brédas, and R. Silbey, in *Quantum Chemistry of Polymers: Solid State Aspects*, edited by J. Ladik, J. M. André, and M. Seel (Reidel, Dordrecht, 1984), p. 221.
[25] R. C. Teitelbaum, S. L. Ruby, and T. J. Marks, J. Am. Chem. Soc. **101**, 7568 (1979); H. Sakai, T. Matsuyama, H. Yamaoka, and Y. Maeda, Bull. Chem. Soc. Jpn. **56**, 1016 (1983); T. Ida, K. Yakushi, and H. Kuroda, J. Chem. Phys. **91**, 3450 (1989).
[26] L. Alcácer and A. H. Maki, J. Phys. Chem. **78**, 215 (1974); **80**, 1912 (1976); R. T. Henriques, M. Almeida, M. J. Matos, L. Alcácer, and C. Bourbonnais, Synth. Met. **19**, 379 (1987); V. Gama, M. Almeida, R. T. Henriques, I. C. Santos, A. Domingos, S. Ravy, and J. P. Pouget, J. Phys. Chem. **95**, 4263 (1991).
[27] H. Akamatu, H. Inokuchi, and Y. Matsunaga, Nature (London) **173**, 168 (1954); Bull. Chem. Soc. Jpn. **29**, 213 (1956).
[28] K. Tanaka, K. Ueda, T. Koike, and T. Yamabe, Solid State Commun. **51**, 943 (1984).
[29] I. Lagerstedt and O. Wennerström, Synth. Met. **20**, 269 (1987).
[30] H. Hartmann and G. Rasch, Acta Polym. **38**, 329 (1987).
[31] A. K. Bakhshi and J. Ladik, Synth. Met. **30**, 115 (1989).
[32] M. Pomerantz, R. Cardona, and P. Rooney, Macromolecules **22**, 304 (1989).
[33] N. Tyutyulkov, A. Tadjer, and I. Mintcheva, Synth. Met. **38**, 313 (1990).
[34] J. J. P. Stewart, J. Comput. Chem. **10**, 209, 221 (1989).
[35] J. J. P. Stewart, MOPAC: A General Molecular Orbital Package (Version 6.0), Q.C.P.E. 455, **10** (1990).
[36] M. J. S. Dewar and W. Thiel, J. Am. Chem. Soc. **99**, 4899 (1977).
[37] M. J. S. Dewar, E. G. Zoebisch, E. F. Healy, and J. J. P. Stewart, J. Am. Chem. Soc. **107**, 3902 (1985).
[38] G. Nicolas and Ph. Durand, J. Chem. Phys. **70**, 2020 (1979); **72**, 453 (1980).
[39] J. M. André, L. A. Burke, J. Delhalle, G. Nicolas, and Ph. Durand, Int. J. Quantum Chem. Symp. **13**, 283 (1979).
[40] J. L. Brédas, R. R. Chance, R. Silbey, G. Nicolas, and Ph. Durand, J. Chem. Phys. **75**, 255 (1981).
[41] E. Ortí and J. L. Brédas, J. Chem. Phys. **89**, 1009 (1988); E. Ortí and J. L. Brédas, Chem. Phys. Lett. **164**, 247 (1989); E. Ortí, J. L. Brédas, and C. Clarisse, J. Chem. Phys. **92**, 1228 (1990); E. Ortí, M. C. Piqueras, R. Crespo, and J. L. Brédas, Chem. Mater. **2**, 110 (1990).
[42] R. Viruela-Martín, P. M. Viruela-Martín, and E. Ortí, J. Chem. Phys. **96**, 4474 (1992).
[43] J. M. André, J. Delhalle, and J. L. Brédas, *Quantum Chemistry Aided Design of Organic Polymers: An Introduction to the Quantum Chemistry of Polymers and its Applications* (World Scientific, Singapore, 1991), Chap. 3.
[44] K. K. Innes, J. E. Parkin, D. K. Ervin, J. M. Hollas, and J. G. Ross, J. Mol. Spectrosc. **16**, 406 (1965).
[45] A. Cammerman and J. Trotter, Proc. R. Soc. London Ser. A **279**, 129 (1964).
[46] J. M. Schulman, R. C. Peck, and R. L. Disch, J. Am. Chem. Soc. **111**, 5675 (1980).
[47] K. A. Kerr, J. P. Ashmore, and J. C. Speakman, Proc. R. Soc. London Ser. A **344**, 199 (1975).
[48] L. H. Scharpen and V. W. Laurie, J. Chem. Phys. **43**, 2765 (1965); G. Liebling and R. Marsh, Acta Crystallogr. **19**, 202 (1965).
[49] K. Tamagawa, T. Iijima, and K. Kimura, J. Mol. Struct. **30**, 243 (1976).
[50] G. Häfelinger and C. Regelmann, J. Comput. Chem. **8**, 1057 (1987); S. Tsuzuki and K. Tanabe, J. Phys. Chem. **95**, 139 (1991).
[51] G. B. Robertson, Nature (London) **191**, 593 (1961); G.-P. Charbonneau and Y. Delugeard, Acta Crystallogr. B **33**, 1586 (1977).
[52] A. Almenningen, O. Bastiansen, L. Fernholt, B. N. Cyvin, S. J. Cyvin, and S. Samdal, J. Mol. Struct. **128**, 59 (1985).
[53] P. A. Clark, F. Brogli, and E. Heilbronner, Helv. Chim. Acta **55**, 1415 (1972).
[54] E. Clar and W. Schmidt, Tetrahedron **33**, 2093 (1977).
[55] E. Clar and W. Schmidt, Tetrahedron **34**, 3219 (1978).
[56] E. Clar and W. Schmidt, Tetrahedron **31**, 2263 (1975); **35**, 2673 (1979).
[57] W. Schmidt, J. Chem. Phys. **66**, 828 (1977).
[58] U. Anton, A. Bohnen, K.-H. Koch, H. Naarmann, H. J. Räder, and K. Müllen, Adv. Mater. **4**, 91 (1992).
[59] E. Clar, *Polycyclic Hydrocarbons* (Academic, London, 1964), Vols. 1 and 2.
[60] J. L. Brédas, B. Thémans, and J. M. André, J. Chem. Phys. **78**, 6137 (1983).
[61] J. L. Brédas, R. R. Chance, R. Silbey, G. Nicolas, and Ph. Durand, J. Chem. Phys. **77**, 371 (1982).
[62] J. L. Brédas, R. R. Chance, R. H. Baughman, and R. Silbey, J. Chem. Phys. **76**, 3673 (1982).